九州大学学術情報リポジトリ
Kyushu University Institutional Repository

DFT Insights into nZVI Reactivity for Environmental Remediation: A Mini Review

Sun Zhaochen
Water and Environmental Engineering Laboratory, Interdisciplinary Graduate School of Engineering Sciences, Kyushu University

Feng Xuening
Water and Environmental Engineering Laboratory, Interdisciplinary Graduate School of Engineering Sciences, Kyushu University

Eljamal, Osama
Water and Environmental Engineering Laboratory, Interdisciplinary Graduate School of Engineering Sciences, Kyushu University

https://doi.org/10.5109/7395754

出版情報：Proceedings of International Exchange and Innovation Conference on Engineering & Sciences (IEICES). 11, pp.1838-1844, 2025-10-30. International Exchange and Innovation Conference on Engineering & Sciences
バージョン：
権利関係：Creative Commons Attribution-NonCommercial-NoDerivatives 4.0 International

KYUSHU UNIVERSITY

DFT Insights into nZVI Reactivity for Environmental Remediation: A Mini Review

Sun Zhaochen[1], Feng Xuening[2], Osama Eljamal[3]

[1]Water and Environmental Engineering Laboratory, Interdisciplinary Graduate School of Engineering Sciences, Kyushu University, 6-1 Kasuga-Koen Kasuga, Fukuoka 816-0933

*Corresponding author email: osama-eljamal@kyudai.jp

Abstract: *This review comprehensively summarizes the application of Density Functional Theory (DFT) in elucidating the reactivity and environmental behavior of nanoscale zero-valent iron (nZVI) for environmental pollution remediation. DFT provides atomic-scale insights into surface reactivity, pollutant adsorption mechanisms, redox transformation pathways, and electronic structure modulation. By modeling interactions between environmental contaminants and Fe surfaces, DFT helps reveal how surface modifications, such as doping and oxidation, influence reactivity and selectivity. We discuss pollutant-specific adsorption configurations, energy barriers for bond activation, and the role of electron transfer processes in degradation. These theoretical findings contribute to the rational design of more efficient, stable, and selective nZVI-based materials. Despite inherent limitations in model simplifications and computational cost, DFT remains a vital tool for bridging molecular mechanisms and material performance, offering strategic guidance for advancing nZVI applications in environmental cleanup and environmental treatment technologies.*

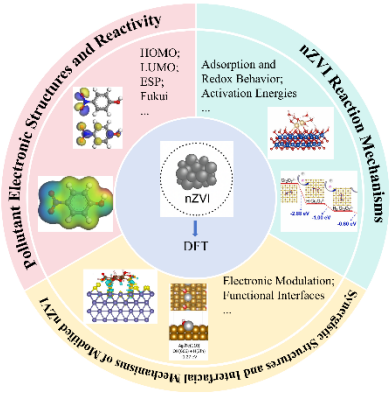

Keywords: Density Functional Theory; nanoscale zero-valent iron; environmental remediation

1. INTRODUCTION

Nanoscale zero-valent iron (nZVI) has become a highly promising material for the remediation of diverse environmental contaminants [1], [35], [36], [37], including heavy metals [2], [38], [39],organic pollutants [3], [40], [41], nitrate [4], [42]. Its high surface area-to-volume ratio, significant reductive capacity, and low cost make it particularly attractive for in-situ applications. However, the mechanisms underlying pollutant adsorption, electron transfer, and surface reactivity are complex and not fully understood, despite its proven effectiveness in environmental remediation.

Traditional experimental techniques often struggle to capture the atomic-level interactions between nZVI and pollutants due to the heterogeneous, reactive, and dynamic nature of nZVI. Over the past years, Density Functional Theory (DFT) has emerged as a valuable computational tool to address this limitation. DFT, a quantum mechanical approach based on the Hohenberg–Kohn theorems and Kohn–Sham formulation, enables the calculation of ground-state properties by solving the Schrödinger equation through electron density, offering a balance of computational efficiency and accuracy. This makes DFT an ideal method for exploring surface reactivity, chemical bonding, and adsorption processes in nanomaterials like nZVI. It enables precise characterization of electronic structures, adsorption energies, reaction pathways, and activation barriers that dictate the pollutant removal behavior of nZVI.

Traditional experimental techniques often struggle to capture the atomic-level interactions between nZVI and pollutants due to the heterogeneous, reactive, and dynamic nature of nZVI. Over the past years, Density Functional Theory (DFT) has emerged as a valuable computational tool to address this limitation. DFT, a quantum mechanical approach based on the Hohenberg–Kohn theorems and Kohn–Sham formulation, enables the calculation of ground-state properties by solving the Schrödinger equation through electron density, offering a balance of computational efficiency and accuracy. This makes DFT an ideal method for exploring surface reactivity, chemical bonding, and adsorption processes in nanomaterials like nZVI. It enables precise characterization of electronic structures, adsorption energies, reaction pathways, and activation barriers that dictate the pollutant removal behavior of nZVI.

While prior reviews have explored the general application of DFT in environmental catalysis, few have systematically integrated its use within a unified theoretical framework focused specifically on nZVI-based materials. To address this gap, this review consolidates recent advances in DFT applications across three critical domains: (1) the elucidation of pollutant degradation mechanisms and redox pathways; (2) the analysis of pollutant electronic structures and reactive sites; and (3) the interfacial mechanisms and synergistic effects introduced by doping and composite modification of nZVI. Finally, the review discusses limitations and perspectives, highlighting DFT's vital role in guiding the rational design of highly efficient and selective nZVI-based materials for environmental remediation.

2. DFT Insights into nZVI Reaction Mechanisms

Understanding the reactivity and surface interactions of nZVI is crucial for optimizing its application in environmental remediation. The mechanisms governing pollutant adsorption and electron transfer are pivotal in determining the material's effectiveness in contaminant removal. These processes can be examined in great detail using Density Functional Theory (DFT), which offers a

molecular-level understanding of the underlying processes.

2.1 Adsorption Behavior

Surface adsorption is often the first critical step in contaminant degradation by nZVI. The strength, orientation, and nature of pollutant adsorption are essential in determining subsequent electron transfer and reactivity. DFT plays a vital role in elucidating these interactions by providing insights into binding energies, charge distributions, and surface coordination geometries.

For heavy metal contaminants, Huang et al.[5] used DFT to investigate the adsorption behavior of Cr(VI) on iron oxides generated from nZVI oxidation. Their results showed that $HCrO_4^-$ exhibited significantly stronger binding to Fe_3O_4 than to FeOOH, a difference attributed to robust Fe–O coordination in Fe_3O_4 and weaker hydrogen bonding interactions in FeOOH. Similarly, Hu et al.[6] applied DFT to compare Cd(II) adsorption on Fe_3O_4(111) and γ-FeOOH(010) surfaces, simulating multiple coordination modes (monodentate, bidentate, tridentate I, tridentate II). They found that Cd(II) favored monodentate adsorption on Fe_3O_4 due to the abundance of isolated hydroxyl groups, whereas γ-FeOOH exhibited lower adsorption capacity because of the prevalence of μ-OH groups. These computational findings are consistent with experimental observations showing reduced Cd(II) removal under aerobic conditions and reveal that Cd(II) can form chain-like structures on γ-FeOOH, promoting surface crystallization. Collectively, these two DFT studies provide a mechanistic understanding at the atomic level for the superior adsorption capacity of Fe_3O_4, underscoring the crucial role of surface phase composition in enhancing the immobilization of heavy metals.

For organic pollutants, Zhang et al. [7], employed DFT calculations to investigate the adsorption behavior of p-nitrophenol (PNP) on various nZVI-derived surfaces. The Fe(110) surface with an LB-30°-2 configuration exhibited strong chemisorption (Ead = −90.53 kcal/mol; Δq = −0.59 e), while FeS demonstrated even stronger binding (Ead = −145.95 kcal/mol; Δq = −0.66 e), attributed to its superior electron transfer capacity and narrow bandgap. In contrast, FeOOH displayed much weaker adsorption (Ead = −17.98 kcal/mol), which was associated with its poor electrical conductivity. Fang et al.[8] explored the adsorption behavior of perfluorinated compounds on nZVI surfaces through DFT calculations, which revealed that PFOS exhibited significantly stronger adsorption (Ead = −5.44 eV) than PFOA (−2.51 eV). The enhanced adsorption of PFOS was attributed to the formation of Fe–S coordination bonds between sulfonic groups and surface iron atoms, as well as greater electron delocalization driven by multiple fluorine atoms. Ghosh et al.[9] investigated the interactions between dye molecules and nZVI surfaces, providing molecular-level insights. For example, eosin yellow (Eo-Y) and erythrosin B (Er-B) were found to exhibit strong hydrogen bonding and dipole–dipole interactions with nZVI surfaces. DFT-calculated chemical hardness (η) values indicated high reactivity for both dyes, with Er-B demonstrating slightly higher reactivity than Eo-Y. These electronic descriptors, combined with adsorption energy calculations, underscore the importance of molecular electron distribution and intermolecular forces in governing adsorption efficiency, further explaining the excellent dye removal performance of nZVI materials. To further elucidate the role of surface doping in regulating adsorption behavior, Che et al. [10] investigated the synergistic effects of sulfide and cellulose nanofiber (TOCNF) modifications in S-nZVI@TOCNF composites designed for trichloroethylene (TCE) degradation. DFT calculations revealed that sulfur doping on the Fe(110) surface markedly reduced the adsorption energies of hydrogen (−0.01 eV) and water molecules (−0.29 eV), indicating a weakened tendency for H and H_2O adsorption and dissociation. This suppression of hydrogen evolution reaction (HER) pathways shifts the surface reactivity toward more selective dechlorination reactions. These results suggest that doping-induced modifications of adsorption energetics can fine-tune the surface chemistry of nZVI, thereby optimizing pollutant selectivity and degradation efficiency. DFT analyses reveal that the adsorption of organic pollutants on nZVI surfaces is jointly governed by the electronic structure of the material (conductivity, bandgap) and the molecular characteristics of the pollutant (functional groups, electron delocalization). Modifying the surface structure and composition of nZVI offers a targeted strategy to optimize adsorption performance for specific organic contaminants.

Overall, DFT analyses of adsorption behavior reveal that adsorption strength is fundamentally governed by the interplay between nZVI surface characteristics and the electronic properties of pollutants. These insights provide a mechanistic basis for rationally tuning surface reactivity and enhancing contaminant removal efficiency.

2.2 Redox Mechanisms and Activation Energies

Beyond adsorption, electron transfer and redox processes govern the efficiency and selectivity of contaminant degradation. DFT provides mechanistic detail on how pollutants are reduced on modified nZVI surfaces.

DFT studies revealed that Cr(VI) reduction on phosphorus-doped nZVI (p-nZVI) occurs via monodentate and bidentate oxygen coordination, with bidentate binding enabling a dual-electron transfer pathway. This enhanced reactivity is supported by EXAFS analysis, indicating a structurally favorable configuration for efficient electron delivery[11]. S-nZVI enables Cr(VI) reduction through a multi-step proton-coupled electron transfer mechanism[12]. Bader charge analysis showed significant electron donation (1.485 e^- to $Cr_2O_7^{2-}$ and 0.948 e^- to $HCrO_4^-$), while projected density of states (PDOS) analysis confirmed orbital hybridization between Fe and Cr. The redox transformation required $6e^-/14H^+$ and $3e^-/7H^+$ per mole, which provided quantitative insight into the electron and proton stoichiometry involved in the reduction process, clarifying the fundamental reaction mechanism. Kong et al.[13] employed DFT simulations to elucidate the redox mechanism underlying V(V) removal by nZVI@LDH. By modeling the adsorption of various vanadium species ($H_2VO_4^-$, VO_2, V_2O_3) on Fe_3O_4(110) surfaces, they found that reduced species V(IV) and V(III) exhibited much stronger adsorption (Eads = −3.46 eV and −5.59 eV) than the oxidized form V(V) (−1.28 eV), indicating enhanced post-reduction stability.

In advanced oxidation processes (AOPs), the reactivity and electron transfer dynamics of nZVI-based catalysts play a pivotal role in the activation of oxidants such as H_2O_2, peracetic acid (PAA), persulfate (PS), sodium persulfate (PDS), potassium monopersulfate (PMS). DFT studies have proven instrumental in uncovering the mechanisms. Zhang et al.[14] designed a novel JCA5Fe@CNs composite by anchoring nZVI onto biomass-derived carbon from waste date palm. DFT calculations were employed to uncover the interfacial redox mechanisms governing H_2O_2 activation in this system. Compared to pristine biochar, JCA5Fe@CNs exhibited significantly stronger adsorption for H_2O_2 and O_2, and lowered the activation energy for H_2O_2 dissociation from 0.52 to 0.18 eV. Bader charge and charge density difference analyses revealed that 0.42 e^- was transferred from nZVI to the carbon matrix, facilitating interfacial electron redistribution. PDOS results further indicated effective orbital hybridization and a decreased work function (2.87 eV), promoting electron mobility. These findings demonstrate that the improved catalytic performance of JCA5Fe@CNs originates from interfacial electronic synergy between nZVI and the biochar carrier, which enhances redox activity and supports reactive oxygen species (ROS) generation via both radical and non-radical pathways. Zhang et al.[15] developed a core–shell structured nZVI@Fe_2P material for the degradation of sulfadiazine (SDZ) and employed DFT simulations to elucidate the underlying redox and electron transfer mechanisms. Compared to the Fe–Fe_2O_3 interface, Fe_2P significantly improved H_2O_2 activation (Eads = −4.54 eV) and enabled dual-direction electron transfer: from Fe^0 to Fe_2P, and from Fe_2P to H_2O_2. Charge density analysis showed that Fe_2P acted both as an electron bridge and donor, promoting •OH generation and maintaining Fe(III)/Fe(II) cycling. The Fe_2P layer also offered better resistance to passivation and could be regenerated with PH_3. These results highlight the role of phosphorus in enhancing electron transfer and long-term catalytic reactivity. This study demonstrates the essential role of DFT in elucidating interfacial electron dynamics, identifying dual-direction electron transfer pathways, and predicting the catalytic reactivity and stability of modified nZVI materials in advanced oxidation processes.

Overall, DFT analyses highlight how electron transfer dynamics, redox site availability, and pathway energetics are directly shaped by material modifications, supporting more efficient and selective contaminant reduction.

3. DFT Insights into Pollutant Electronic Structures and Reactivity

While the reactivity of nZVI-based materials is essential for pollutant degradation, the intrinsic electronic structure of contaminants also critically influences their susceptibility to oxidation, reduction, and radical attack. To elucidate the molecular basis of this reactivity, numerous studies have employed Density Functional Theory (DFT) to investigate the frontier molecular orbitals, charge distribution, and reactive sites of pollutants, thereby uncovering their degradation pathways in both nZVI and nZVI-activated advanced oxidation processes (AOPs). Table 1 compiles the DFT analysis of representative cases of organic pollutant degradation mechanisms.

DFT serves as a powerful tool to explore these molecular characteristics, enabling accurate prediction of degradation pathways and identification of the most reactive atomic sites. Specifically, frontier molecular orbitals (the HOMO and LUMO) indicate a molecule's propensity to donate or accept electrons, while charge distribution and electrostatic potential (ESP) analyses reveal regions susceptible to electrophilic or nucleophilic attack. Furthermore, Fukui functions and related reactivity descriptors help pinpoint atoms most prone to transformation. These computational descriptors collectively provide a mechanistic foundation for understanding and predicting the environmental fate of complex organic pollutants under various treatment conditions.

Sulaiman et al. [16] investigated the adsorption of bisphenol A (BPA) on nZVI surfaces, demonstrating through HOMO–LUMO isosurface analysis that electron-rich moieties such as hydroxyl and phenyl groups act as donors, with a net electron transfer (ΔN = 0.70) toward the iron surface. This directional electron flow underscored a donor–acceptor chemisorption mechanism. Similarly, Fan et al. [17] applied frontier orbital and electrostatic potential (ESP) analysis to p-nitrophenol (PNP), revealing that the nitro and hydroxyl groups were key electrophilic targets under oxidative conditions, thus explaining its reactivity with hydroxyl radicals in AOPs.

Further insights were obtained by Ye et al. [18], who examined atrazine (ATZ) using advanced descriptors such as $2FED^2HOMO$ and $FED^2HOMO+LUMO$ to identify oxidation-prone atoms in a sulfidated nZVI/peroxydisulfate system. Their findings correlated well with LC–MS-detected intermediates, offering a clear molecular-level explanation of degradation pathways. Wu et al. [19] extended this integrative approach to metronidazole (MNZ), combining Fukui function and ESP mapping to locate active sites like O17, C2, and N14, which were consistent with experimentally verified pathways involving ring opening and hydroxylation. In another example, Pei et al. [20] explored N-nitrosopyrrolidine (NPYR) and identified O15, N13, and N14 as highly reactive via condensed Fukui indices and dual descriptor analysis, linking electronic vulnerability with observed bond cleavage and radical attack. The degradation mechanism of clothianidin (CTD) was clarified through LUMO energy level calculations and Fukui f^+ analysis, which jointly indicated that nitro groups were more susceptible to nucleophilic reduction than chlorinated positions. This theoretical evidence aligned with observed transformation products[21].

Antibiotic degradation has also been elucidated using DFT methods. Zhao et al. [22] examined florfenicol (FF) in the NZVI@MIL-53(Al)/H_2O_2 system, where HOMO orbitals and Fukui function values identified key reactive sites (e.g., C1, C3, O17, Cl19) susceptible to electrophilic and radical attack, supporting degradation routes involving hydroxylation, dehalogenation, and peptide bond cleavage. For tetracycline (TC), Duan et al. [23] integrated Fukui function analysis, average local ionization energy (ALIE), and electrostatic potential (ESP) mapping to comprehensively assess the molecule's reactivity. The computational results indicated that aromatic carbon atoms and adjacent functional groups

were particularly susceptible to electrophilic and radical attacks. These predicted reactive sites closely matched the LC–MS-identified pathways of ring-opening and functional group loss.

Collectively, DFT enables detailed identification of molecular reactive sites, supports the proposal of degradation pathways, and complements experimental validation, thereby advancing the mechanistic understanding of pollutant removal in environmental systems.

Table I. DFT Analysis of Organic Pollutant Degradation Mechanisms

Pollutant	Material/System	DFT Method	Key Reaction Sites	Degradation Mechanism	Reference
Bisphenol A	nZVI	HOMO/LUMO; Fukui functions	isopropyl moiety, phenyl rings, and hydroxyl groups	Donor-acceptor-based chemisorption	[16]
Clothianidin	S-nZVI-BC	HOMO/LUMO; Fukui functions	Nitro groups	Preferential nitro reduction, detoxification	[21]
p-nitrophenol	SnZVI@GO-PS	HOMO/LUMO; ESP	Hydroxyl and nitro groups	Electrophilic attack-driven oxidation	[17]
Atrazine	S-nZVI/PDS	HOMO/LUMO; charge distribution	Specific carbon and nitrogen atoms	Electron transfer-induced oxidation and radical attack	[18]
metronidazole	nZVI/Cu^0/BC/PMS	Fukui function	O16, O15, C1-C3, N14, N17	Hydroxylation, N-O bond cleavage, ring-opening	[24]
N-Nitrosopyrrolidine	Cu-nZVI/PS	HOMO/LUMO; Fukui functions	N13, N14, O15	Radical-induced N–N and N–O bond cleavage	[20]
tetracycline	WS-AC/nZVI/PMS	HOMO/LUMO; Fukui functions; ESP	C2, C4, C6, C-O, C-N	Aromatic and functional group cleavage	[23]
florfenicol	NZVI@MIL-53(Al)/H_2O_2	HOMO/LUMO; Fukui functions; charge distribution	The benzene ring carbons (C1-C6) and C11; O17, Cl19, C3	·OH-induced cleavage of peptide and sulfonic groups	[22]
2,4-dichlorophenol	Fe/Ni-CMC-PS	HOMO/LUMO; charge distribution	Phenolic hydroxyl, aromatic ring, Cl positions	Electrophilic/nucleophilic attack on aromatic ring and Cl	[25]
metronidazole	Fe^0@CQDs-TiO_2(b)	HOMO/LUMO; Fukui functions; ESP	C2, C3, C4, C5, N19, O17, O21	Primarily aromatic ring cleavage	[19]
chloramphenicol	S-nZVI/PS	Fukui functions	O17, O16, N15	·OH radical attack at active sites, dechlorination and denitration	[26]
tetracycline hydrochloride	Fe^0@Fe_2O_3/YC/PMS	HOMO/LUMO	Aniline group, hydroxyl group	Deamidation, dealkylation, oxidation	[27]

4. DFT Insights into Synergistic Structures and Interfacial Mechanisms of Modified nZVI

Beyond pristine nanoscale zero-valent iron (nZVI), Density Functional Theory (DFT) studies have provided detailed insights into the interfacial reaction mechanisms and structural modifications of various enhanced nZVI-based materials. These computational investigations underscore the significance of surface regulation, dopant incorporation, and functional group modification in improving pollutant adsorption, reduction behavior, and overall reactivity. Recent DFT-based investigations have underscored the pivotal role of surface structural regulation and functional group engineering in enhancing the reactivity and selectivity of modified nZVI materials for pollutant removal. These modifications, especially in composite systems, create favorable interfacial environments that improve adsorption affinity, promote electron transfer, and facilitate redox reactions.

4.1 Doping modification and Electronic Modulation

DFT modeling has been instrumental in elucidating how sulfur doping influences nZVI reactivity.

White et al. [28]conducted a comprehensive DFT study to investigate how doping nZVI with transition metals (Pd, Ni, Cu, Ag) alters its surface properties and reactivity toward contaminant removal. By simulating Fe(110), Fe(211), and Fe(210) crystal surfaces, they demonstrated that dopant incorporation was thermodynamically more favorable at low-coordination sites, especially on stepped Fe(210) and Fe(211) facets. Among the dopants, Pd consistently accepted electrons from neighboring Fe atoms, as shown by Bader charge and PDOS analysis, leading to enhanced redox potential. In contrast, the electronic modulation of Cu, Ni, and Ag was found to be surface-dependent. Furthermore, Pd and Ag weakened water adsorption, particularly in dissociative modes, suggesting improved corrosion resistance. Ni-doped surfaces exhibited stronger hydrogen adsorption, indicating suitability for hydrogen-mediated degradation pathways, whereas Pd promoted weak hydrogen binding and desorption, favoring redox-driven pollutant transformation. Overall, Pd was identified as the most effective dopant, providing a balance between surface stabilization, electron transfer enhancement, and corrosion suppression. This study exemplifies how DFT modeling enables atomic-level understanding of dopant-induced surface modifications, guiding the rational design of bimetallic nZVI for advanced environmental applications.

The coordination mode of Cr(VI) transforms from monodentate (Ead = −1.25 eV) on pristine nZVI to bidentate (Ead = −2.24 eV) on phosphorus-doped nZVI, reflecting enhanced adsorption and reduction efficiency through shortened Fe–Cr distances[11].

Similarly, sulfidated nZVI (FeS model) demonstrates significantly improved adsorption affinity for Cr(VI), with $Cr_2O_7^{2-}$ showing a strong binding energy of −5.11 eV, substantially higher than that of $HCrO_4^-$ (−2.29 eV). The moderate interaction with the reduction product $Cr(OH)_3$ (−2.75 eV) suggests that sulfidation also facilitates product stabilization post-reduction [12]. Che et al. [10] demonstrated through DFT that sulfur incorporation shifts surface charge distribution—sulfur gained −0.54 e while Fe became more electropositive (+0.13 e). This redistribution weakened Fe–H interactions and reinforced Fe–Cl bonding, thereby enhancing TCE dechlorination while inhibiting HER. These findings collectively highlight that sulfur doping not only alters the thermodynamics of surface reactions but also improves contaminant specificity by electronically tailoring the nZVI interface.

Expanding on these insights, Choe et al. [29] investigated the electronic modulation effects of sulfur on Fe(110) surfaces. Their DFT results revealed that sulfur doping significantly reduced the binding energies of H^+ and H_2O (−0.898 eV and −0.02 eV, respectively), thereby suppressing hydrogen evolution reactions (HER) and water-induced passivation. This suppression increased the availability of surface electrons for NO_3^- reduction. Complementary electrochemical and XPS data confirmed that S-doped nZVI (notably $S_{0.125}$ZVI) exhibited improved Fe solubility, elevated Fe(II) content, and enhanced electron transfer efficiency, ultimately increasing the selectivity for N_2 formation. Further supporting these findings, Brumovský et al. [30] used DFT to study trichloroethene (TCE) reduction on sulfidated vs. pristine Fe. While initial sulfur doping inhibited reactivity, mirroring sulfur poisoning in metal catalysts, subsequent surface corrosion transformed S atoms into catalytically active sites. These sites not only protected adjacent Fe atoms but also facilitated selective electron transfer toward TCE reduction. This dynamic evolution underscores sulfur's dual role in suppressing undesired side reactions while promoting target pollutant reduction under realistic conditions. Zhen et al. [31] deepened this mechanistic understanding by combining DFT and EXAFS analyses. Their study showed that sulfur atoms, strongly stabilized on Fe(110) surfaces (E_ads = −5.91 eV), inhibited H and H_2O adsorption. Charge density difference maps revealed electron accumulation near sulfur sites, contributing to HER suppression and directing electrons preferentially toward pollutant reduction. Experimental validation using tert-butyl alcohol (TBA) confirmed that sulfur doping enhanced selective dechlorination of fluorinated phenols (FF) by mitigating radical competition from HER.

DFT studies highlight that doping modification effectively enhances the reactivity, selectivity, and stability of nZVI by precisely tuning its electronic structure and reaction pathways.

4.2 Support modification and Functional Interfaces

Support modification has emerged as a powerful strategy for enhancing the performance of nZVI in pollutant removal, by engineering surface structure, tuning electronic properties, and promoting interfacial reactivity. Functional interfaces enable improved dispersion, electron transfer efficiency, contaminant selectivity, and catalytic durability. DFT-based investigations have been instrumental in elucidating the mechanistic underpinnings of these enhancements.

NZVI supported on MBenes exhibited strong binding interactions with Cr(VI) and U(VI), with adsorption energies reaching −8.64 eV for $HCrO_4^-$ and −4.85 eV for UO_2^{2+}. These high affinities were attributed to surface functional groups that promoted interfacial electron redistribution, supported OH-bond cleavage, and facilitated stable immobilization of heavy metals [32]. Liu et al.[33] developed a zero-valent iron-loaded corn straw biochar (ZVI-CSC) that showed enhanced adsorption of As(V) and reduced its leaching in soil, while the improvement for Cd(II) was limited. DFT calculations were used to analyze the effects of different surface functional groups on metal adsorption. ESP and bond dissociation enthalpy (BDE) analyses indicated that hydroxyl groups had the strongest affinity for As(V), C–O–C groups favored Cd(II) binding, and C=O and –COOH groups could simultaneously bind both metals. DFT directly revealed the relationship between functional group types and metal binding behavior, providing a theoretical basis for tuning interfacial chemistry to enhance selective adsorption. Similarly, Zhang et al. [14] demonstrated that biochar-supported nZVI (JCA5Fe@CNs) significantly lowered the activation energy for H_2O_2 decomposition (from 0.52 eV to 0.18 eV). DFT-derived Bader charge analysis confirmed a 0.42 e^- electron transfer from Fe to the carbon support, while partial density of states (PDOS) analysis indicated enhanced orbital hybridization, both contributing to improved redox activity. Qureashi et al. [34] further confirmed that porous biochar enhanced glyphosate adsorption and facilitated interfacial electron

transfer in nZVI composites, with DFT revealing the strong contribution of surface functional groups to binding affinity and electrochemical performance.

Notably, Zhou et al. provided deep insights into the role of 2D material supports by studying MoS_2-supported nZVI (nZVI@MD). Their DFT simulations revealed that Fe doping and sulfur vacancies in MoS_2 induced lattice distortions that generated local potential fields, enhancing electron mobility. Compared to pristine MoS_2, nZVI@MD exhibited metallic conductivity, a higher density of states near the Fermi level, and a reduced work function (0.205 Ha vs. 0.227 Ha), all of which facilitated efficient electron transfer and pollutant reduction. Additionally, lower O_2 adsorption energies and higher H_2O affinity supported its superior oxidative stability and reactivity.

Collectively, DFT-based investigations underscore the pivotal role of DFT in understanding how support materials and surface functionalization synergistically modulate the interfacial electronic environment of nZVI, offering a theoretical foundation for the rational design of advanced and stable composites for environmental remediation.

5. REFERENCES

[1] Yi, L. and O. Eljamal, Mini review on the application research of nanoscale zero valent iron in water treatment. 2023.

[2] Yang, M.Y., X.Y. Zhang, and Y.C. Sun, Remediation of Cr(VI) Polluted Groundwater Using Zero-Valent Iron Composites: Preparation, Modification, Mechanisms, and Environmental Implications. Molecules, 2024. **29**(23): p. 21.

[3] Xue, W.J., et al., Affecting factors and mechanism of removing antibiotics and antibiotic resistance genes by nano zero-valent iron (nZVI) and modified nZVI: A critical review. Water Research, 2024. **253**: p. 17.

[4] Shiotsuki, M. and O. Eljamal. The Effect of Aging nZVI on Removal of Nitrate. 2024. International Exchange and Innovation Conference on Engineering & Sciences.

[5] Huang, X., et al., Fate and mechanistic insights into nanoscale zerovalent iron (nZVI) activation of sludge derived biochar reacted with Cr(VI). J Environ Manage, 2022. **319**: p. 115771.

[6] Hu, Y.B., et al., Insights into the mechanisms of aqueous Cd(II) reduction and adsorption by nanoscale zerovalent iron under different atmosphere conditions. J Hazard Mater, 2022. **440**: p. 129766.

[7] Zhang, J., et al., Removal of p-nitrophenol by double-modified nanoscale zero-valent iron with biochar and sulfide: Key factors and mechanisms. Journal of Water Process Engineering, 2023. **51**.

[8] Fang, J., et al., Selective perfluorooctanoic acid (PFOA) and perfluorooctane sulfonate (PFOS) adsorption by nanoscale zero-valent iron (nZVI): performance and mechanisms. Environmental Science: Nano, 2024. **11**(5): p. 1915-1925.

[9] Ghosh, S., et al., Liquid-phase adsorption modeling of Eosin Y and Erythrosin B dyes onto nanoscale zero-valent iron using response surface and computational methodologies. Sustainable Water Resources Management, 2023. **9**(5): p. 160.

[10] Che, M., et al., A Kirkendall strategy for the efficient degradation of trichloroethylene from groundwater using cellulose nanofiber-supported sulfidated nZVI. Chemical Engineering Journal, 2024. **501**.

[11] Li, M., et al., Phosphate modification enables high efficiency and electron selectivity of nZVI toward Cr(VI) removal. Applied Catalysis B: Environmental, 2020. **263**.

[12] Wang, Y., et al., Processes and mechanisms in remediation of aqueous chromium contamination by sulfidated nano-scale zerovalent iron (S-nZVI): Experimental and computational investigations. J Hazard Mater, 2024. **469**: p. 134031.

[13] Kong, X., et al., Enhanced removal of vanadium(V) from groundwater by layered double hydroxide-supported nanoscale zerovalent iron. J Hazard Mater, 2020. **392**: p. 122392.

[14] Zhang, M., et al., A novel environmentally friendly catalyst for the preparation and degradation of DNT in dynamite wastewater: Performance, mechanism and application. Environ Res, 2025. **276**: p. 121488.

[15] Zhang, X., et al., Novel core-shell structural nZVI@Fe2P for sulfadiazine (SDZ) degradation: Accelerated Fe(III)/Fe(II) dynamic cycling, boosted Fenton performance and stability. Separation and Purification Technology, 2024. **347**.

[16] Sulaiman, W.K., et al., Exploring zero-valent iron nanoparticles (nZVI) for Bisphenol A removal: Experimental investigations and Monte-Carlo simulation insights. Water Practice & Technology, 2024. **19**(8): p. 3416-3438.

[17] Fan, X., et al., Graphene oxide supported S-nZVI to activate persulfate for effective degradation of p-nitrophenol: Performance, mechanism and toxicity evolution. Journal of Water Process Engineering, 2025. **72**.

[18] Ye, Z., et al., Revealing the degradation of atrazine in S-nZVI/peroxydisulfate system with density functional theory calculation. Journal of Water Process Engineering, 2025. **71**.

[19] Wu, X., et al., Exceptional photo-elimination of antibiotic by a novel Z-scheme heterojunction catalyst composed of nanoscale zero valent iron embedded with carbon quantum dots (CQDs)-black TiO(2). J Hazard Mater, 2023. **460**: p. 132323.

[20] Pei, Y., et al., Efficient activation of persulfate by copper-coated nano zero-valent iron for degradation of nitrogenous disinfection by-products: The key role of Cu. J Colloid Interface Sci, 2025. **684**(Pt 1): p. 213-225.

[21] Li, F., et al., Optimizing FeS crystallinity of sulfidated nZVI to enhance electron transport capacity for clothianidin efficient degradation: Regulation of biochar pyrolysis temperature. J Hazard Mater, 2025. **487**: p. 137256.

[22] Zhao, Z., et al., Investigation of the degradation and dehalogenation properties of florfenicol by heterogeneous Fenton reaction activated with MIL-53(Al)-supported nano zero-valent iron. Chemical Engineering Journal, 2023. **453**.

[23] Duan, P., et al., Peroxymonosulfate activation by walnut shell activated carbon supported nano zero-valent iron for the degradation of tetracycline: Performance, degradation pathway and mechanism. Environ Res, 2024. **245**: p. 117971.
[24] Xu, W., et al., Biochar encapsulated metal nanoflowers for high efficient degradation of metronidazole via peroxymonosulfate activation. Separation and Purification Technology, 2024. **328**.
[25] Zhao, Y., et al., Degradation of 2,4-dichlorophenol by carboxymethylcellulose stabilized Fe/Ni activating persulfate system: The DFT calculation and mechanistic insights. Journal of Environmental Chemical Engineering, 2023. **11**(6).
[26] Wu, G., et al., Removal of chloramphenicol by sulfide-modified nanoscale zero-valent iron activated persulfate: Performance, salt resistance, and reaction mechanisms. Chemosphere, 2022. **286**(Pt 3): p. 131876.
[27] Li, B., et al., In-situ preparation of yeast-supported Fe(0)@Fe(2)O(3) as peroxymonosulfate activator for enhanced degradation of tetracycline hydrochloride. Chemosphere, 2023. **324**: p. 138340.
[28] White, J.J., et al., The impact of metal dopants on the properties of nZVI: a theoretical study. Journal of Physics: Materials, 2024. **7**(1).
[29] Choong, C.E., et al., Hydrophobic sulfur core–shell layered metallic iron for nitrate reduction with nearly 100% dinitrogen selectivity: Mechanism and field studies. Chemical Engineering Journal, 2023. **454**.
[30] Brumovsky, M. and D. Tunega, Intrinsic Effects of Sulfidation on the Reactivity of Zero-Valent Iron With Trichloroethene: A DFT Study. J Phys Chem C Nanomater Interfaces, 2023. **127**(43): p. 21063-21074.
[31] Cao, Z., et al., Unveiling the Role of Sulfur in Rapid Defluorination of Florfenicol by Sulfidized Nanoscale Zero-Valent Iron in Water under Ambient Conditions. Environ Sci Technol, 2021. **55**(4): p. 2628-2638.
[32] Liu, F., et al., Immobilizing nZVI particles on MBenes to enhance the removal of U(VI) and Cr(VI) by adsorption-reduction synergistic effect. Chemical Engineering Journal, 2023. **454**.
[33] Liu, B., et al., Remediation of As(V) and Cd(II) Contamination by a ZVI-Biochar: Experimental and DFT Calculation. Water, Air, & Soil Pollution, 2024. **235**(1): p. 74.
[34] Qureashi, A., et al., Electrochemical analysis of glyphosate using porous biochar surface corrosive nZVI nanoparticles. Nanoscale Adv, 2023. **5**(3): p. 742-755.
[35] O. Eljamal, K. Sasaki, T. Hirajima, Sorption kinetic of arsenate as water contaminant on zero valent iron, J. Water Resour. Prot. 5 (2013) 563–567.
[36] O. Eljamal, J. Okawauchi, K. Hiramatsu, Removal of phosphorus from water using marble dust as sorbent material, J. Environ. Prot. 3 (2012) 709–714.
[37] B. Singha, S.C. Karmaker, O. Eljamal, Quantifying the direct and indirect effect of socio-psychological and behavioral factors on residential water conservation behavior and consumption in Japan, Resour. Conserv. Recycl. 190 (2023) 106816.
[38] O. Eljamal, R. Eljamal, O. Falyouna, I. Maamoun, I.P. Thompson, Exceptional contribution of iron nanoparticle and Aloe vera biomass additives to biogas production from anaerobic digestion of waste sludge, Energy 263 (2024) 131761.
[39] I. Maamoun, R. Eljamal, O. Eljamal, Statistical optimization of nZVI chemical synthesis approach towards P and NO_3^- removal from aqueous solutions: Cost-effectiveness & parametric effects, Chemosphere 312 (2023) 137176.
[40] O. Falyouna, I. Maamoun, K. Bensaida, A. Tahara, Y. Sugihara, O. Eljamal, Chemical deposition of iron nanoparticles (Fe^0) on titanium nanowires for efficient adsorption of ciprofloxacin from water, Water Pract. Technol. 17 (2022) 75–83.
[41] O. Falyouna, I. Maamoun, S. Ghosh, A. Malloum, A. Othman, O. Eljamal, T.W.M. Amen, A. Oroke, C. Bornman, S. Ahmadi, M.H. Dehghani, A.H. Mahvi, S. Nasseri, I. Tyagi, J.R. Koduru, Sustainable technologies for the removal of chloramphenicol from pharmaceutical industries effluent: A critical review, J. Mol. Liq. 368 (2022) 120726.
[42] T.W.M. Amen, O. Eljamal, A. Khalil, N. Matsunaga, Evaluation of sulfate-containing sludge stabilization and the alleviation of methanogenesis inhibition at mesophilic temperature, J. Water Process Eng. 25 (2018) 212–221.